Plant Physiol. (1995) 107: 725–735

Effects of Iron Excess on *Nicotiana plumbaginifolia* Plants[1]

Implications to Oxidative Stress

Karlheinz Kampfenkel, Marc Van Montagu*, and Dirk Inzé

Laboratorium voor Genetica (K.K., M.V.M.) and Laboratoire Associé de l'Institut National de la Recherche Agronomique (France) (D.I.), Universiteit Gent, B-9000 Gent, Belgium

Fe excess is believed to generate oxidative stress. To contribute to the understanding of Fe metabolism, Fe excess was induced in *Nicotiana plumbaginifolia* grown in hydroponic culture upon root cutting. Toxicity symptoms leading to brown spots covering the leaf surface became visible after 6 h. Photosynthesis was greatly affected within 12 h; the photosynthetic rate was decreased by 40%. Inhibition of photosynthesis was accompanied by photoinhibition, increased reduction of photosystem II, and higher thylakoid energization. Fe excess seemed to stimulate photorespiration because catalase activity doubled. To cope with cellular damage, respiration rate increased and cytosolic glucose-6-phosphate dehydrogenase activity more than doubled. Simultaneously, the content of free hexoses was reduced. Indicative of generation of oxidative stress was doubling of ascorbate peroxidase activity within 12 h. Contents of the antioxidants ascorbate and glutathione were reduced by 30%, resulting in equivalent increases of dehydroascorbate and oxidized glutathione. Taken together, moderate changes in leaf Fe content have a dramatic effect on plant metabolism. This indicates that cellular Fe concentrations must be finely regulated to avoid cellular damage most probably because of oxidative stress induced by Fe.

Fe is an essential element for many proteins involved in cellular processes of higher plants, most notably photosynthesis and respiration. Despite this, many aspects of Fe metabolism, such as phloem loading and unloading, intracellular transport (e.g. uptake in mitochondria and chloroplasts), storage, and homeostasis, are largely unknown. This holds true for both the physiology and the molecular biology of Fe metabolism. Only Fe uptake in roots has received more attention. However, although the principle of the uptake route by dicots has been known for more than 20 years, namely that soil Fe^{3+} chelates are reduced at the root surface to Fe^{2+}, which is the actual uptake form (Chaney et al., 1972), none of the involved transport proteins has yet been identified at the protein or cDNA level.

Clearly, Fe metabolism should be adapted to the cellular demands. Whereas Fe deficiency results in chlorosis, Fe excess is believed to generate oxidative stress (Halliwell and Gutteridge, 1984). Toxic reduced O_2 species are inevitable by-products of biological oxidations. The toxicity of the relatively unreactive superoxide radicals and H_2O_2 arises by the Fe-dependent conversion into the extremely reactive hydroxyl radicals (Haber-Weiss reaction) that cause severe damage on membranes, proteins, and DNA (Halliwell and Gutteridge, 1984). Because hydroxyl radicals are by far too reactive to be controlled directly, aerobic organisms eliminate the less reactive O_2 species as efficiently as possible. H_2O_2 is removed by catalases, AsA peroxidases, and GSH peroxidases. The dismutation of superoxide radicals to O_2 and H_2O_2 is catalyzed by metal-containing SODs (Bowler et al., 1992).

Recently, evidence that Fe uptake leads to an oxidative stress has been acquired for *Escherichia coli* and yeast. Indeed, genes coding for both Fe uptake and oxidative stress response are regulated by the same transcription factors in these organisms. *E. coli* has uptake systems for Fe^{3+} chelates (Kampfenkel and Braun, 1993) and Fe^{2+} (Kammler et al., 1993). The transport genes are repressed under conditions of Fe sufficiency by the Fur repressor protein that is activated through binding to Fe^{2+} (Braun and Hantke, 1990). The Fur protein serves also as a transcriptional regulator of *sodA* (coding for MnSOD) and *sodB* (FeSOD) (Fee, 1991). In the eukaryote *Saccharomyces cerevisiae*, Fe uptake requires, as in roots of dicots, a reduction step and the subsequent translocation of Fe^{2+} across the cytoplasmic membrane via a still unknown transport protein. The expression of the *FRE1* gene, coding for the transmembrane Fe^{3+} reductase of yeast, is repressed by Fe (Dancis et al., 1992). The transcription factor MAC1 is necessary for the basal transcription level of *FRE1* and for the feedback

[1] This research was supported by grants from the Belgian Programme on Interuniversity Poles of Attraction (Prime Minister's Office, Science Policy Programming, No. 38), the "Vlaams Actieprogramma Biotechnologie" (ETC 002), and the International Atomic Energy Agency (No. 5285). D.I. is a Research Director of the Institut National de la Recherche Agronomique (France). K.K. is indebted to the Deutsche Forschungsgemeinschaft (Germany) for a postdoctoral fellowship.

* Corresponding author; e-mail mamon@gengenp.rug.ac.be; fax 32-9-2645349.

Abbreviations: AsA, ascorbate; DAsA, dehydroascorbate; F_m, fluorescence yield with a saturating pulse in dark-adapted material; F_o, ground fluorescence obtained by using a weak non-actinic modulated beam in the dark; G6PDH, glucose-6-phosphate dehydrogenase; NADP-MDH, malate dehydrogenase (NADP dependent); Q_A, the primary acceptor site of PSII; qQ, photochemical quenching; qNP, nonphotochemical quenching; SOD, superoxide dismutase.

regulation by elevated Fe. Most noteworthy, MAC1 is also involved in the transcription of *CTT1*, which encodes the cytosolic catalase (Jungmann et al., 1993).

The aim of this work was to investigate whether the uptake of Fe leads to an oxidative stress in plants, thus necessitating a co-regulation of Fe uptake and oxidative stress response. Here, we describe a new means of approaching this problem. This method takes advantage of plant growth in hydroponic culture and the very rapid infiltration of any kind of water-soluble toxic compound upon partial root cutting via the transpiration stream. By measuring photosynthesis, respiration, Chl fluorescence parameters, carbohydrates, extractable activity of selected enzymes, and levels of antioxidants, we show that moderate increases in the leaf Fe content have a dramatic effect on overall plant metabolism.

MATERIALS AND METHODS

Plant Material and Growth Conditions

Seeds of *Nicotiana plumbaginifolia* L. were incubated overnight in 0.05% (w/v) GA_3 solution and germinated on vermiculite moistened with saturated $CaSO_4$ solution. After 10 d, seedlings were separated, grown in saucers filled with vermiculite, and supplied with nutrition solution. After 14 d, the plantlets were transferred to allow hydroponic culture. Plants were grown in an aerated nutrient solution of pH 5.6 containing $Ca(NO_3)_2$ (2.0 mM), K_2SO_4 (0.7 mM), $MgSO_4$ (0.5 mM), KCl (0.1 mM), and KH_2PO_4 (0.1 mM) as macronutrients and H_3BO_3 (10 μM), $MnSO_4$ (0.5 μM), $ZnSO_4$ (0.5 μM), $CuSO_4$ (0.2 μM), and $(NH_4)_6Mo_7O_{24}$ (0.01 μM) as trace elements. Fe was supplied as 30 μM Fe(III)-EDTA (sodium salt; Fluka Chemie AG, Buchs, Switzerland).

For hydroponic culture, plants were grown in rectangular polyethylene containers (60 × 16 cm, 12 cm deep) containing 7.5 L of nutrient solution. Nutrient solutions were changed every 10 d and transpiration losses were replenished every 2 d. After 10 d, the pH had increased by 1.6 ± 0.1 units (mean ± SD, n = 8), depending on the plant age. Plants were grown in a controlled environment chamber: 24 to 26°C, 16 h light, 8 h dark, 130 μmol m^{-2} s^{-1} light intensity at the level of the lowest leaf, and 45 to 55% RH.

Induction of Fe Excess and Plant Harvest

Seven- to 8-week-old plants of uniform size were selected. At this stage the plants were about 25 cm tall and had formed an immature inflorescence. Only middle-aged, unshaded leaves of comparable size were harvested. The smallest and largest leaves used were 10 and 18 cm long, respectively. Fe excess was induced upon root cutting in the presence of fresh nutrient solution containing 100 μM Fe(III)-EDTA and 100 μM additional $MgSO_4$ (pH of the final solution was 6.3). When the roots had been cut, control plants were placed in nutrient solution without Fe but with, instead, 100 μM $MgSO_4$ and 100 μM Na_2-EDTA. These were supplied from a 0.1 M stock of $MgSO_4$ and Na_2-EDTA adjusted to pH 6.3 to allow Mg-EDTA complex formation. Upon root cutting, a second set of control plants was placed in a fresh solution without Fe but with 100 μM $MgSO_4$ (pH 6.3). Roots were cut at the beginning of the light period by removing two-thirds of the root length with a scalpel.

Twelve hours after the roots were cut, four to six leaves of each plant were harvested. Three to five leaf discs of 1.3 cm diameter were collected from each leaf using a cork borer to determine fresh weight and Chl content. The rest of the leaves were divided in halves by removing the middle ribs. One part of these halves was shock-frozen in liquid N_2 and stored at −80°C until analysis. The other part was weighed and subsequently subjected to Fe determination. Four control and four Fe excess plants were analyzed separately for each parameter.

Fe Content Determination

Leaf material equivalent to 5 to 11 g fresh weight was dried in an oven at 60°C overnight, weighed, and dry ashed overnight in a muffle oven at 500°C. The ash was dissolved in a beaker with 20 mL of hot (70°C) 3 M HNO_3 and wet digested by boiling for 30 min. Evaporation losses were continuously replenished by adding hot 3 M HNO_3. After 30 min, the solution was filtered through a blue band filter (type 589[3]; Schleicher & Schuell, Dassel, Germany) in a volumetric flask. Beakers were washed several times with hot 3 M HNO_3 and the filters were subsequently rinsed twice with 5 mL of double-distilled water. Digests were analyzed for Fe directly or after additional dilution with 1% (v/v) HNO_3 by atomic spectroscopy using a SpetrAA-10 spectrophotometer (Varian Analytical Instruments, San Fernando, CA) and standard Fe solutions.

Enzyme Determinations

About 0.4 to 0.6 g of frozen leaf material was ground to a fine powder in a prechilled mortar. The powder was extracted in 1 mL of 50 mM Hepes (pH 7.4), 5 mM $MgCl_2$, 1 mM EDTA, 1 mM EGTA, 0.1% (v/v) Triton X-100, 1 mM PMSF, 4 mM benzamidine, 4 mM 6-aminocaproic acid by vortexing until completely thawed. Aliquots (100 μL) were frozen in liquid N_2 until assayed. Thawed extracts were centrifuged for 5 min at 15,600g (4°C), and aliquots of the supernatant equivalent to 1.5 to 3.5 μg of Chl were used for enzyme activity measurements. Activity was assayed at 25°C by following the A change in a 1-mL reaction mixture using a UV-160A spectrophotometer (Shimadzu Scientific Instruments, Columbia, MD).

Catalase activity was measured as described by Cakmak and Marschner (1992). AsA peroxidase was determined as described by Klapheck et al. (1990). GSH peroxidase was measured according to the method of Drotar et al. (1985). Corrections were made for the GSH peroxidase activity present as impurity in the commercially available GSH reductase from yeast (type III from bakers yeast; Sigma). SOD activity was measured with the nitroblue tetrazolium-based assay as described by Beyer and Fridovich (1987). Linearization of the SOD inhibited nitroblue tetrazolium reduction and definition of 1 SOD unit was entirely as

described by Giannopolitis and Ries (1977) using increasing amounts of crude extract. G6PDH measurements were carried out as described by Graeve et al. (1994). To approximate the chloroplastic G6PDH activity, a sample was preincubated for 10 min at room temperature in 0.1 M Tris-HCl (pH 8.0), 62.5 mM DTT. NADP-MDH was activated by incubation of the sample with 0.1 M Tris-HCl (pH 8.0), 62.5 mM DTT at room temperature for 10 min prior to the determination of enzyme activity. Activity was assayed as described by Kampfenkel (1992).

Chl, Pheophytin, and Protein Determination

Chl content was measured according to the method of Arnon (1949). Pheophytin was determined after acid extraction with 6% (w/v) TCA or 10% (v/v) $HClO_4$ as described by Hipkins and Baker (1986). Soluble protein was estimated with a colorimetric assay using a bicinchoninic acid/$CuSO_4$ mixture (Smith et al., 1985) according to the supplier's instructions (Sigma). BSA served as a standard. Total protein was obtained using aliquots of the enzyme extract (see above) brought to 1.0% (v/v) Triton X-100 to solubilize membrane proteins during a 30-min incubation period at room temperature with slight shaking. Insoluble material and membranes were subsequently sedimented by centrifugation at 15,600*g* for 30 min. The supernatant was assayed by the detergent-insensitive bicinchoninic acid/$CuSO_4$ method (Smith et al., 1985).

IEF and SOD Activity Stain

IEF with aliquots of the enzyme extracts (see above) using Ampholine PAG plates (pH 4–6.5; Pharmacia, Uppsala, Sweden) was performed with the MultiphorII electrophoresis unit (Pharmacia) as recommended by the supplier. SOD activity was assayed on IEF gels using the in situ staining technique of Beauchamp and Fridovich (1971).

Determination of Soluble Sugars and Starch

Leaf discs were taken at different times, lyophilized, homogenized with an electric drill, and extracted in 500 μL per disc of 80% (v/v) ethanol (10 mM Hepes-KOH [pH 7.8], 1 mM $MgCl_2$) at 80°C for 4 min with vigorous shaking as described by Sonnewald et al. (1991). The supernatant obtained after 10 min at 15,600*g* was used for the enzymatic determination of Glc, Fru, and Suc as described by Stitt et al. (1989). The pellet was washed with 1 mL of ice-cold water. The sediment was then resuspended in 200 μL of 100 mM sodium-acetate buffer (pH 4.7) and autoclaved for 2 h at 125°C. Subsequently, 5 units/mL of amylase and amyloglucosidase (Boehringer Mannheim, Germany) were added and incubated for 2 h at 37°C with shaking. After the sample was heat inactivated (95°C for 3 min) and centrifuged (10 min at 15,600*g*), the supernatant was subjected to Glc determination as described by Stitt et al. (1989).

Gas Exchange and Chl Fluorescence Measurements

Samples (two leaf discs from two plants per experiment, diameter 3.5 cm) were removed from selected areas of the leaves 12 h after root cutting and the plants continued to grow in the light. Two experiments per treatment were performed. Photosynthesis and respiration were measured at 15°C in a leaf disc O_2 electrode (Hansatech, Kings Lynn, UK) modified for simultaneous measurements of O_2 evolution and Chl fluorescence. CO_2 was supplied from 400 μL of 2 M carbonate buffer (pH 9.2) containing 5 units/mL carbonic anhydrase. The plant material was predarkened for 30 min prior to the measurements.

Chl fluorescence was measured with a PAM Chl fluorescence measuring system (Walz, Effeltrich, Germany) using actinic light of 570 μmol m^{-2} s^{-1} and a 800-ms pulse of saturating light of 2600 μmol m^{-2} s^{-1} to differentiate between the qQ and the qNP. The F_o was measured using a 1.6-kHz measuring beam with an irradiance of less than 0.1 μmol m^{-2} s^{-1}. All estimates of qQ and qNP in steady state were related to F_o as described by Schreiber et al. (1986).

Metabolite Measurements

AsA and DAsA were determined according to the method of Okamura (1980) with modifications for leaf tissue. Frozen leaf material (0.4–0.8 g) was ground to a fine powder in a prechilled mortar and 0.8 mL of 6% (w/v) TCA was added. The frozen TCA was reduced to a fine powder. The mixture was continually homogenized until completely thawed, allowed to stand for 15 min on ice, and centrifuged in 2-mL reaction vessels for 5 min at 15,600*g* (4°C). The clear supernatant was immediately assayed. Total AsA (AsA plus DAsA) was measured after reduction of DAsA with DTT. Concentrations of DAsA were calculated from the difference of total AsA and AsA (without pretreatment with DTT). The reaction medium for total AsA contained 0.2 mL of the supernatant and 0.6 mL of 0.2 M phosphate buffer (pH 7.4), 10 mM DTT. After a 15-min incubation in a water bath at 42°C, 0.2 mL of 0.5% (w/v) *N*-ethylmaleimide was added to remove excess DTT. Incubation lasted for 1 min at room temperature. The reaction mixture for AsA contained 0.2 mL of the supernatant, 0.6 mL of 0.2 M phosphate buffer (pH 7.4), and 0.2 mL of double-distilled H_2O. In both reaction mixtures, the color was developed after addition of 1 mL of 10% (w/v) TCA, 0.8 mL of 42% (v/v) *o*-phosphoric acid, 0.8 mL of 4% (w/v) α,α′-dipyridyl (dissolved in 70% [v/v] ethanol), and 0.4 mL of 3% (w/v) $FeCl_3$. Mixtures were incubated in a water bath at 42°C for 40 min and subsequently the A_{525} was read. Corrections were made for color development in the absence of sample. AsA and DAsA (both from Sigma) were dissolved in 6% (w/v) TCA and used for calibration.

GSH and GSSG were assayed as described by Griffith (1980) with slight modifications. Frozen leaf material (0.2–0.4 g) was ground to a fine powder in a prechilled mortar, and 0.8 mL of 10% (v/v) $HClO_4$ was added. The frozen $HClO_4$ was ground to a fine powder and the mixture continually homogenized until completely thawed. After incubation on ice for 15 min the precipitated protein was removed by centrifugation, and the supernatant was neutralized by successive addition of 1 M triethanolamine, 5 M KOH according to the method of Stitt et al. (1989). The

resulting $KClO_4$ precipitate was removed by centrifugation for 5 min at 15,600*g* (4°C). The clear supernatant was assayed immediately. To assay for GSSG, endogenous GSH was masked with 2-vinylpyridine. The supernatant (450 μL) was mixed vigorously with 9 μL of 2-vinylpyridine for 1 min and subsequently incubated for 1 h at 30°C in a water bath. Total GSH (GSH and GSSG) and GSSG were measured in a 1-mL reaction volume containing 0.2 mL of sample and 0.8 mL of 125 mM phosphate buffer (pH 7.5), 6.3 mM EDTA, 0.26 mM NADPH, and 0.75 mM 5,5′-dithiobis(2-nitrobenzoic acid). Upon the addition of 0.5 unit of GSH reductase (type III from baker's yeast; Sigma), the change in A_{412} was recorded for 3 min at 30°C using a HP8452A Diode Array spectrophotometer (Hewlett-Packard, Palo Alto, CA). The GSH content of the sample was determined by comparison of the rate of 5,5′-dithiobis(2-nitrobenzoic acid) reduction observed to standard curves generated with known amounts of GSH and GSSG (both from Sigma). Reduced GSH was determined as the difference between total GSH and GSSG.

Recoveries for all measured metabolites were estimated by extraction of leaf material in the presence of a standard mixture containing a 2- to 3-fold excess over the endogenous metabolites and subsequent analysis. Recoveries were: AsA, 73 ± 5%; DAsA, 105 ± 2%; GSH, 95 ± 11%; GSSG, 99 ± 10% (mean ± SD, n = 4). Recoveries were proven to be the same for control and Fe-stressed leaf material (data not shown).

RESULTS

Effects of Fe Excess on Plant Growth

Fe excess was induced upon root cuttings, two-thirds of the root were removed, and hydroponic growth was continued in the presence of 100 μM Fe(III)-EDTA and in the light. All visible phenotypes described below were independent of the plant age (from two-leaf stage to flowering) and were always the same based on observations of about 100 plants. To elucidate any effect by EDTA, control plants were treated when the roots were cut with a nutrient solution containing additional 100 μM Mg-EDTA in the absence of Fe. In a second set of control plants, the effect of only 100 μM additional $MgSO_4$ in the absence of Fe was analyzed. After 6 h, the Fe-treated plants showed slight symptoms of toxicity by uptake of Fe from the nutrient solution via the transpiration stream. Leaves were covered with some faint spots 2 to 3 mm in diameter that appeared next to the veins. Some leaves showed a bright surface, indicating water loss by disruption of leaf tissue. After 9 h, the spots became more numerous and slightly larger and started to cover the whole leaf surface. Twelve hours after the roots were cut, all leaves were covered with small brown spots. In addition, some larger and irregularly shaped yellow patches appeared between the veins. After 12 h, none of the control plants showed any visible phenotype. Whereas the Fe excess phenotype was only slightly more pronounced after 24 h, now also some of the control plants (10–20%) treated with Mg-EDTA showed a few necrotic spots (Fig. 1, A and B). However, these few spots were qualitatively different, appeared only on a small number of control plants, and always appeared later than the Fe toxicity symptoms. In addition, this Mg-EDTA phenotype remained unchanged even after extended growth for 5 d (data not shown). Control plants treated with 100 μM $MgSO_4$ were indistinguishable from wild type (Fig. 1, A and B) even after 5 d (data not shown). Figure 1C shows plants 5 d after roots were cut and treated with Fe. The very young leaves were green and unaffected. This was due to the repair of the root damage within the first 24 to 48 h, allowing controlled uptake of nutrients again and, thus, normal Fe supply to the young developing leaves. Recutting of the roots resulted in the same Fe excess phenotype of these leaves (data not shown). Figure 1D shows in greater detail two Fe-stressed leaves after 5 d. Because of partial shading two sectors were less affected. However, this was not indicative of a light-dependent Fe toxicity but rather of a reduced transpiration of the shaded areas and thus reduced uptake of Fe. This was concluded from leaf disc experiments. Dark incubation of leaf discs in the presence of 1 mM Fe(III)-EDTA led to the same visible symptoms of Fe toxicity after 24 h (data not shown).

To be sure that the described toxicity phenotype was related to an increase in the leaf Fe content, Fe concentrations were determined for control and Fe excess plants after 12 h. Indeed, the leaf Fe content doubled from 0.29 ± 0.03 to 0.65 ± 0.07 μg cm^{-2} in the Fe-stressed plants (Table I). Whereas the leaves of *N. plumbaginifolia* plants treated with 100 μM Fe(III)-EDTA for 12 h already showed severe morphological signs of Fe toxicity, there were nearly none or only slight differences in fresh weight, dry weight, and Chl, soluble protein, and total protein content compared to the control (Table I).

Carbohydrates, O_2 Exchange, and Chl Fluorescence

The control plants grown upon root cuttings in the presence of 100 μM Mg-EDTA had a much higher total leaf carbohydrate pool (starch plus Suc plus hexoses) than the Fe-stressed plants (Table II) at the end of the light periods (16 and 40 h). The ratio of soluble sugars (Suc and hexoses) to starch was strongly decreased in the Fe-treated leaves compared to the control. This was due to a relatively larger decrease in free hexoses than in starch (Table II). Suc contents remained nearly unchanged. At the end of the dark period upon root cuttings (24 h), the content of free hexoses was much higher compared to that at the onset of the preceding light period (0 h) in both control and Fe-stressed leaves (Table II).

The CO_2-saturated rate of photosynthesis at low light intensities was decreased by 40% in the Fe-stressed leaves after 12 h (Fig. 2). Under light saturation the photosynthetic rate was reduced from 126 to 86 μmol O_2 h^{-1} mg^{-1} Chl. In marked contrast, the respiration rate of the darkened leaves was nearly doubled after 12 h of Fe stress when compared with control plants treated with 100 μM Mg-EDTA for 12 h and increased from 4.4 to 7.9 μmol O_2 h^{-1} mg^{-1} Chl. The photosynthesis and respiration rates were well within the range reported for *N. plumbaginifolia* (Foyer et al., 1994).

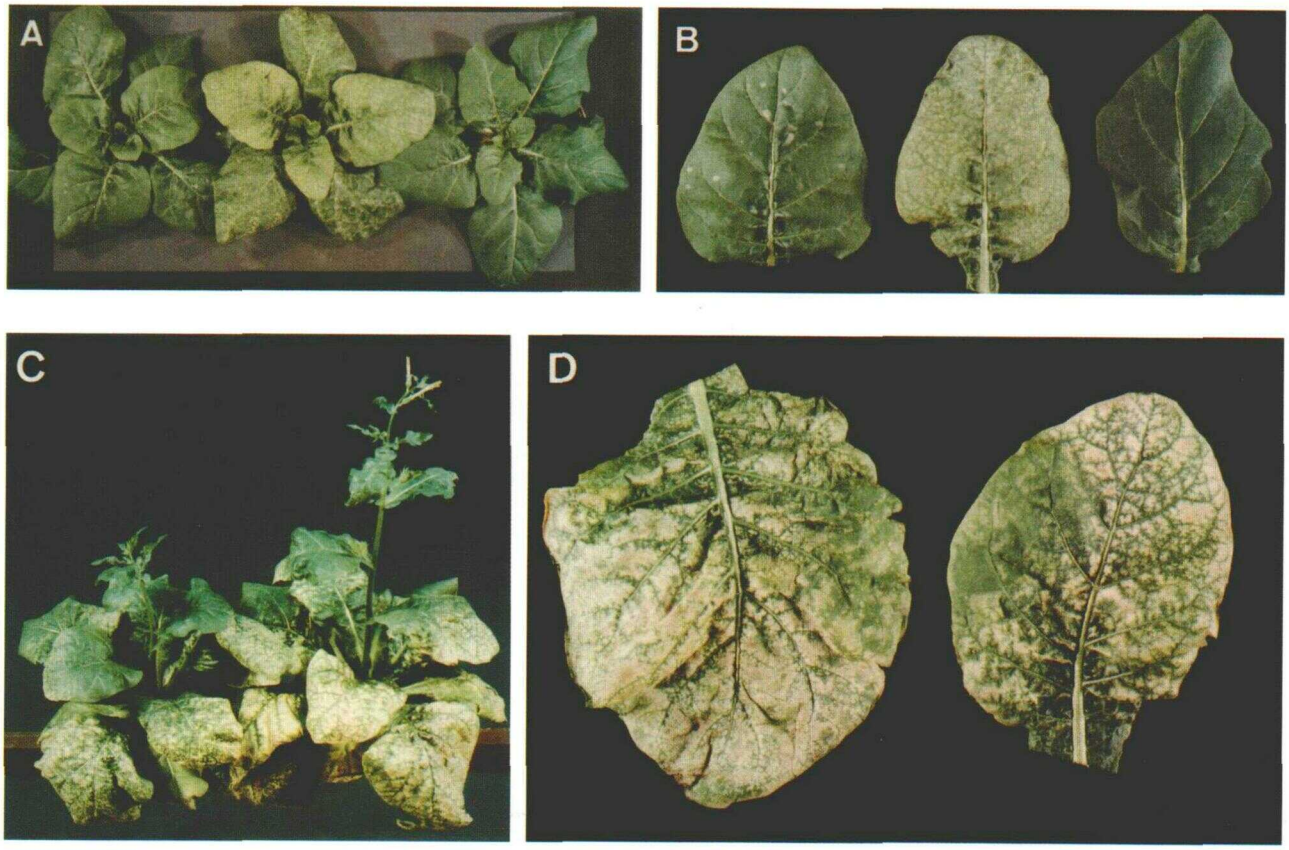

Figure 1. Phenotype of Fe excess plants. Symptoms were independent of plant age. A, Six-week-old plants in the rosette stage grown after their roots had been cut for 24 h (see "Materials and Methods") in the presence of 100 μM Mg-EDTA (left), 100 μM Fe(III)-EDTA (middle), and 100 μM additional $MgSO_4$ (right). Note that all treatments were performed in a nutrient solution without Fe (see "Materials and Methods"). B, Detailed view of leaves from the same plants as in A. C, Nine-week-old plants grown after their roots had been cut for 5 d in the presence of 100 μM Fe(III)-EDTA. Note unaffected young leaves and flowers. D, Two leaves from the same plants as in C. Note less damaged sections due to reduced transpiration by partial shading. After 5 d, the visible phenotype of the Mg-EDTA-treated plants was indistinguishable from the appearance after 24 h (data not shown).

Three different Chl fluorescence parameters (F_m/F_o ratio, qQ, and qNP) were measured to provide insight into the response of the photosynthetic electron transport. A decrease in the F_m/F_o ratio indicates that the leaf has been photoinhibited (Björkman and Powles, 1984). Light-exposed control leaves had an F_m/F_o ratio of 5.0, which is typical for unstressed leaf material. The F_m/F_o ratio of the Fe-stressed leaves was decreased to 4.1, showing that photoinhibition occurred after 12 h. The qQ is a measure for the reduction state of Q_A (Schreiber et al., 1986). Under all light intensities, Q_A was more strongly reduced by about 10% in the Fe-stressed leaves (Fig. 3A). This shows that the inhibition of photosynthesis is accompanied by increased reduction of PSII. The qNP is composed of several components (Quick and Stitt, 1989). Even under low light intensities, qNP was increased by 40 to 60% in the Fe-treated leaves compared to the control (Fig. 3B). This indicates that Fe-induced inhibition of photosynthesis is accompanied by a higher thylakoid energization.

All measured Chl fluorescence parameters of the control plants were identical with those previously reported for unstressed *N. plumbaginifolia* wild-type plants (Foyer et al., 1994).

Activities of Oxidative Stress-Responsive Enzymes

The effect of 12 h of Fe excess on the specific activities of catalase, AsA peroxidase, GSH peroxidase, SOD, and G6PDH in leaves is shown in Figure 4. Both catalase and AsA peroxidase activities nearly doubled within 12 h of Fe stress. The specific activity of catalase increased from 0.005 $\pm$ 0.001 μmol min^{-1} mg^{-1} protein in the control to 0.009 $\pm$ 0.001 μmol min^{-1} mg^{-1} protein in the Fe-stressed leaves. The AsA peroxidase activity increased from 0.88 $\pm$ 0.15 to 1.70 $\pm$ 0.22 μmol min^{-1} mg^{-1} protein. There were no significant changes in GSH peroxidase and SOD activities (Fig. 4). The changes were most pronounced for G6PDH; the Fe excess-exposed leaves contained 2- to 3-fold higher activity than the control leaves (from 0.010 $\pm$ 0.003 to 0.026 $\pm$ 0.005 μmol min^{-1} mg^{-1} protein; Fig. 4).

In vitro, the chloroplast G6PDH can be inactivated by a reductant such as DTT (Johnson, 1972). In contrast, the

Table I. *Evolution of various plant parameters for control and Fe excess-exposed plants*

Fresh weight, dry weight, and Chl, soluble protein, total protein, and Fe contents were determined in control plants treated with 100 μM Mg-EDTA and Fe excess-exposed plants 12 h after root cuttings as described in "Materials and Methods." Data are mean values ± SD from four measurements (10 measurements in the case of fresh weight). Dry weight and Fe content were determined only once per plant. For each parameter average values ± SD are indicated based on analysis of four individual control and four individual Fe excess-exposed plants.

Plant	Fresh Wt	Dry Wt	Chl	Soluble Protein	Total Protein	Fe Content	Soluble Protein/Chl	Total Protein/ Soluble Protein
	$\mu g\ cm^{-2}$	$\mu g\ cm^{-2}$	$\mu g\ cm^{-2}$	$\mu g\ cm^{-2}$	$\mu g\ cm^{-2}$	$\mu g\ cm^{-2}$		
Control plants								
C1	27.74 ± 6.68	2.09	29.9 ± 2.9	199.2 ± 3.3	365.8 ± 12.1	0.27	6.7	1.8
C2	34.89 ± 7.00	2.16	25.1 ± 1.8	174.1 ± 4.9	304.6 ± 23.8	0.26	6.9	1.7
C3	33.61 ± 4.51	2.21	29.2 ± 2.3	277.6 ± 13.2	495.9 ± 29.6	0.32	9.5	1.8
C4	33.68 ± 6.62	2.20	27.2 ± 3.2	149.8 ± 10.3	412.6 ± 20.6	0.31	5.5	2.8
Mean	32.48 ± 3.21	2.17 ± 0.05	27.9 ± 2.2	200.2 ± 55.4	394.7 ± 80.7	0.29 ± 0.03	7.2 ± 1.7	2.0 ± 0.5
Fe excess plants								
+1	27.59 ± 5.99	2.17	31.1 ± 3.8	198.8 ± 18.7	415.5 ± 16.0	0.76	6.4	2.1
+2	35.71 ± 4.42	2.38	28.4 ± 3.8	163.6 ± 17.3	363.2 ± 34.2	0.63	5.8	2.2
+3	30.30 ± 6.16	2.15	29.5 ± 3.3	265.0 ± 20.0	549.0 ± 42.5	0.60	9.0	2.1
+4	25.26 ± 3.88	1.92	31.4 ± 4.7	189.0 ± 9.9	463.7 ± 36.0	0.62	6.0	2.5
Mean	29.72 ± 4.50	2.16 ± 0.19	30.1 ± 1.4	204.1 ± 43.2	447.9 ± 78.9	0.65 ± 0.07	6.8 ± 1.5	2.2 ± 0.2

cytosolic G6PDH is not inactivated by DTT (Graeve et al., 1994). This different behavior can be used to approximate the relative activities of the cytosolic and chloroplastic G6PDH upon preincubation with DTT (see "Materials and Methods"). In both control and Fe excess-exposed samples, the G6PDH activity remained unchanged after incubation with DTT (data not shown). As a positive control the activity of NADP-MDH, another chloroplast enzyme that is activated in vitro by DTT, was measured (Kampfenkel, 1992). Whereas the nontreated sample showed no measurable NADP-MDH activity, the activity was increased after incubation with DTT to 0.056 ± 0.005 $\mu mol\ min^{-1}\ mg^{-1}$ protein. This result indicated that the DTT pretreatment used should have been sufficient to also reduce chloroplastic G6PDH. Because the G6PDH activity remained unchanged in control and Fe-stressed samples after incubation in the presence of DTT, it can be concluded that either the chloroplastic enzyme cannot be detected in a crude extract because of low abundance or that the chloroplastic G6PDH is extremely unstable (Graeve et al., 1994). Taken together, these results suggest that the increase in G6PDH activity under Fe excess conditions is mainly if not exclusively due to the cytosolic G6PDH.

Several SOD forms contribute to the measurable total SOD activity in a crude leaf extract (Bowler et al., 1992). Therefore, it was possible that a decrease of one SOD form was masked by a compensatory increase in another form. The levels of individual SOD isoforms were assessed by subjecting extracts of leaf samples of the four control and four Fe excess-exposed plants to IEF and subsequent activity staining on a gel. The activity stain revealed three bands of SOD activity in leaf samples of *N. plumbaginifolia* (Fig. 5). Inhibition studies with H_2O_2 and KCN, routinely used to distinguish between Cu/Zn-, Mn-, and FeSOD (Bowler et al., 1989), showed that the upper faint band was an MnSOD (resistant to H_2O_2 and KCN), the middle band was an FeSOD (resistant to KCN and sensitive to H_2O_2), and the lower band was a Cu/ZnSOD (sensitive to H_2O_2 and KCN) (J. Kurepa, personal communication). Other SOD bands could not be detected. Figure 5 clearly shows that there were no significant changes in the levels of individual SOD isoenzymes.

Table II. *Carbohydrate contents of leaves from control and Fe-stressed plants measured at different times after root cutting*

Measurements were at the beginning of the light period (0 h), the end of the light period (16 h), the end of the dark period (24 h), and the end of the following illumination period (40 h). Light intensity was 130 $\mu mol\ s^{-1}\ m^{-2}$. Data are means ± SD from four different control and four different Fe excess-exposed plants. ΣC_6, Total sum of hexose equivalents.

Sample	Time of Harvest	Metabolite Contents					Soluble Sugar/ Starch Ratio
		Glc	Fru	Suc	Starch	ΣC_6	
	h	*nmol hexose* cm^{-2}					
Control	0	20 ± 5	19 ± 2	3 ± 1	132 ± 50	174	0.32
	16	225 ± 29	306 ± 69	13 ± 1	659 ± 263	1203	0.83
	24	83 ± 35	138 ± 84	3 ± 1	85 ± 70	309	2.64
	40	139 ± 33	198 ± 46	11 ± 1	666 ± 241	1014	0.52
Fe excess	0	20 ± 5	20 ± 12	3 ± 1	174 ± 56	217	0.25
	16	62 ± 12	102 ± 34	10 ± 2	495 ± 275	669	0.35
	24	45 ± 7	94 ± 4	3 ± 1	176 ± 83	318	0.81
	40	41 ± 8	51 ± 11	11 ± 4	516 ± 105	619	0.20

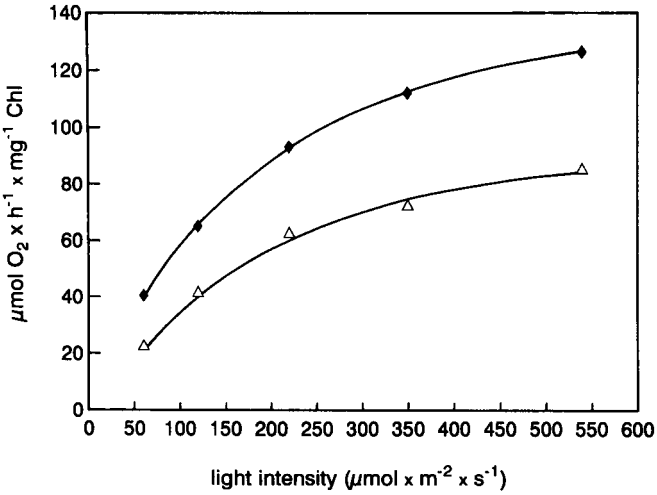

Figure 2. Effect of light intensity on the rate of O_2 evolution in control leaves (♦) and Fe-treated leaves (△). Measurements were performed under saturating CO_2 12 h after roots had been cut as described in "Materials and Methods." Representative results are shown.

Effect of Fe Excess on Antioxidant Levels

Metabolite levels were compared in control leaves and Fe-stressed leaves 12 h after the roots had been cut and continued to grow in the light (Table III). Both control and Fe-treated leaves of individual plants, although of uniform size and grown under identical conditions, showed large deviations in the endogenous levels of AsA, DAsA, GSH, and GSSG. However, based on the average values, within 12 h Fe excess led to a decrease in both the AsA content (from 0.86 ± 0.20 to 0.59 ± 0.15 μmol g^{-1} fresh weight) and GSH content (from 0.25 ± 0.10 to 0.18 ± 0.12 μmol g^{-1} fresh weight) of 30%. At the same time, this resulted, taking the recoveries into account, in equivalent increases of the DAsA and GSSG contents (Table III). The endogenous DAsA level in control plants was below the detection limit of 0.04 μmol g^{-1} fresh weight of the assay used (see "Materials and Methods"). Also the GSSG content in control leaves was very low at 0.01 ± 0.004 μmol g^{-1} fresh weight (Table III). Apparently, there was no net increase in the total amounts of AsA and DAsA or of GSH and GSSG after 12 h of Fe excess.

DISCUSSION

A method was developed to allow rapid infiltration of Fe(III)-EDTA in plant tissue. We circumvented the root uptake system by partial removal of the roots. This permitted uncontrolled uptake of water-soluble compounds simply via the transpiration stream in the light. To evaluate any toxic effect by EDTA, we chose *N. plumbaginifolia* plants as a control, which were placed after the roots had been cut in a nutrient solution without Fe but with 100 μM Mg-EDTA instead. Although after 24 h about 20% of these control plants developed a few necrotic spots on their leaves (Fig. 1A), this can be discounted on the basis of several physiological parameters that indicated that these plants behaved like untreated plants. Respiration rate, photosynthesis rate (Fig. 2), qQ and qNP (Fig. 3), soluble protein/Chl ratio (Table I), and carbohydrate content (Table II) were nearly identical with the values obtained by Foyer et al. (1994) for *N. plumbaginifolia* wild-type plants. This can also be concluded from the redox states of the AsA/DAsA and GSH/GSSG couples. They are known for the close relative *N. tabacum* to be strongly reduced in unstressed leaf material (Foyer et al., 1991). Indeed, in the control plants used here, the GSH/GSSG couple was reduced to 96%, and for the AsA/DAsA the oxidized form could not even be detected (Table III). This demonstrates that the control was not particularly stressed by the root cutting or by the presence of 100 μM Mg-EDTA.

Addition of 100 μM Fe(III)-EDTA to hydroponically grown *N. plumbaginifolia* plants upon root cutting led to visible toxicity symptoms after 6 h, finally resulting in faint brown and necrotic spots covering the whole leaf surface (Fig. 1). Within 12 h, the Fe content of leaves was doubled, indicating that this phenotype was caused by excess Fe (Table I). A similar phenotype has been described for an Fe-overaccumulating pea mutant (Kneen et al., 1990) that had about a 60-fold higher leaf Fe content compared to wild type (Welch and LaRue, 1990). This Fe excess phenotype of pea has been investigated in more detail by means of light microscopy and EM (Guinel and LaRue, 1990). This

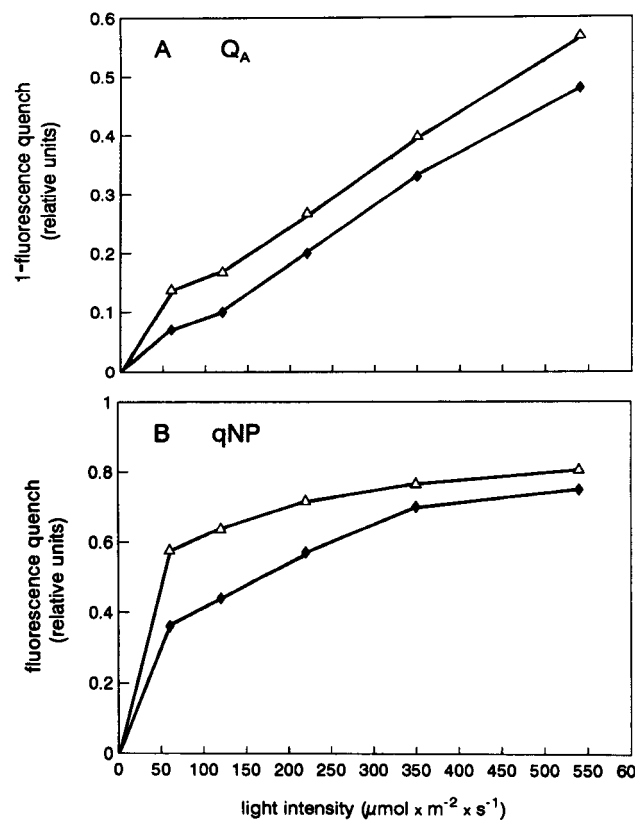

Figure 3. Curves of Q_A reduction (A) and qNP (B) in response to light measured under saturating CO_2 in the same experiment as shown in Figure 2. Control leaves (♦) and Fe-stressed leaves (△). Representative results are shown.

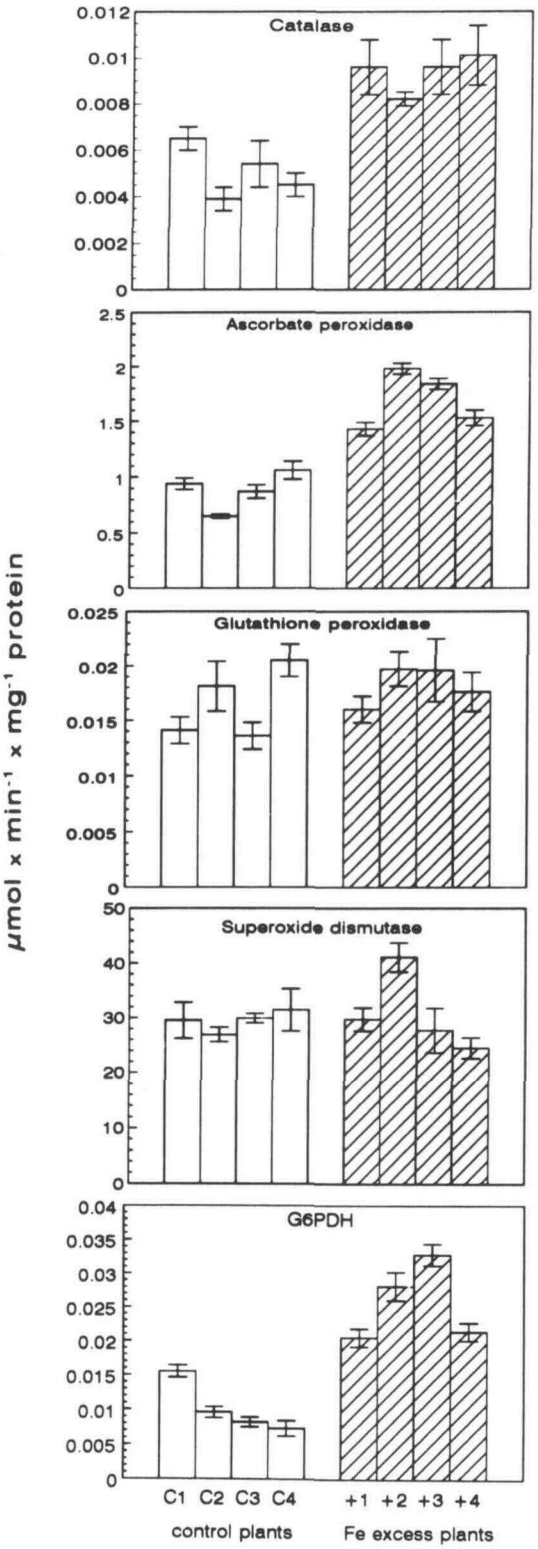

Figure 4. Catalase, AsA peroxidase, GSH peroxidase, SOD, and G6PDH activities of control leaves (plants C1–C4) and Fe-stressed leaves (plants +1 to +4) assayed 12 h after roots had been cut. Enzyme activities are expressed as μmol min^{-1} mg^{-1} protein with the exception of SOD activity, which is presented as units mg^{-1} protein. For SOD unit definition, see "Materials and Methods." Results are means ± SD (n = 4).

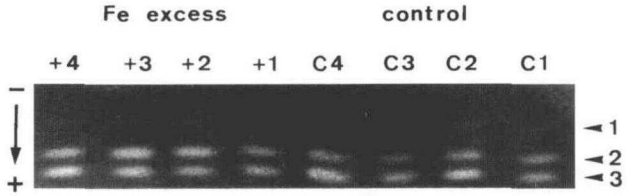

Figure 5. *SOD activity stain on gel after IEF of leaf sample (15 μg of protein each) from four control (C1–C4) and four Fe excess plants (+1 to +4). The same extracts were used as in Figure 4. 1, MnSOD; 2, FeSOD; 3, Cu/ZnSOD.*

study revealed large cell wall appositions in the living cells surrounding the dead material of the necrotic spots and small dense inclusions in vacuoles of mesophyll cells. The last observation is very interesting in light of findings by Raguzzi et al. (1988), who showed that vacuoles are involved in the storage of Fe in yeast cells. Based on these observations, it is an attractive working hypothesis that excess Fe may be somehow sequestered in these developing necrotic spots and in vacuoles of mesophyll cells. However, the intracellular distribution of Fe and the detoxification of excess Fe by higher plants is unknown.

Although there were no major differences in fresh weight, dry weight, or Chl, soluble protein, and total protein contents of the Fe-stressed leaves compared to controls (Table I), Fe excess clearly had a dramatic effect on photosynthesis within 12 h. An increase of the leaf Fe content decreased the CO_2-saturated photosynthesis rate by 30 to 40% (Fig. 2) and the amount of starch at the end of the light periods by 25% under ambient conditions (Table II). Inhibition of photosynthesis was also revealed by the increased energization of the thylakoid membrane, increased reduction state of PSII, and induced photoinhibition (Fig. 3). The observed inhibition was primarily due to an impairment of the photosynthetic electron transport and/or coupling caused by Fe but not to a direct inhibition of end product (starch and Suc) synthesis. This can be concluded from the kinetics of the light-response curves of CO_2-saturated photosynthesis rate (Fig. 2), reduction state of Q_A (Fig. 3A), and qNP (Fig. 3B), which showed significant changes already at very low light intensities. At low light, the CO_2-saturated photosynthesis rate was decreased by 40%, the Q_A was more strongly reduced, and the qNP was increased by 60%. Similar kinetics have been observed by Neuhaus and Stitt (1989) by perturbing the rate of photosynthetic electron transport with methyl viologen, acting as an alternative electron acceptor at the acceptor site of PSI, or tentoxin, which inhibits the CF_1 ATP synthase. An inhibition of end product synthesis results in other changes that are clearly different from those reported here. Inhibition of both Suc and starch synthesis is also accompanied by an inhibition of the CO_2-saturated photosynthesis, increased Q_A reduction, and higher qNP but only at high light intensities with little or no changes at low light (Neuhaus et al., 1989; Neuhaus and Stitt, 1991). As a whole, these results strongly suggest that the increase of the leaf Fe content to toxic levels led to an increased uptake of Fe in chloroplasts and, thus, a dramatic impairment of the total photosynthetic

Table III. *Effect of Fe on the endogenous levels of AsA, DAsA, GSH, and GSSG as measured 12 h after root cutting*

The analyses were performed as described in "Materials and Methods." Mean values ± SD ($n = 4$). For each metabolite, the average values ± SD are indicated based on analysis of four control and four Fe excess-exposed plants.

Plant	Metabolite Content			
	AsA	DAsA	GSH	GSSG
	μmol g⁻¹ fresh wt			
Control plants				
C1	0.95 ± 0.05	ND[a]	0.43 ± 0.04	0.007 ± 0.002
C2	0.53 ± 0.03	ND	0.19 ± 0.01	0.008 ± 0.001
C3	0.87 ± 0.03	ND	0.18 ± 0.03	0.009 ± 0.001
C4	1.07 ± 0.03	ND	0.21 ± 0.03	0.015 ± 0.001
Mean	0.86 ± 0.23		0.25 ± 0.12	0.010 ± 0.004
Fe excess-exposed plants				
+1	0.52 ± 0.02	0.22 ± 0.04	0.06 ± 0.01	0.051 ± 0.007
+2	0.38 ± 0.03	0.24 ± 0.02	0.06 ± 0.004	0.046 ± 0.005
+3	0.70 ± 0.01	0.31 ± 0.04	0.31 ± 0.01	0.020 ± 0.003
+4	0.75 ± 0.02	0.47 ± 0.02	0.29 ± 0.02	0.032 ± 0.002
Mean	0.59 ± 0.17	0.31 ± 0.11	0.18 ± 0.14	0.037 ± 0.014

[a] Not detectable with this assay. Detection limit for DAsA is 0.04 μmol g^{-1} fresh weight.

electron transport capacity by unknown means. However, at the moment we do not know whether this indicates that chloroplasts are involved in the detoxification of excess Fe. We should point out that the Fe acquisition strategy of chloroplasts is completely unknown.

The Calvin cycle inhibition caused by Fe through impairment of the photosynthetic electron transport chain might decrease the carboxylation/oxygenation ratio of the Rubisco reaction, thus favoring photorespiration. Fixation of O_2 by Rubisco is the primary event in this metabolic sequence, which leads to the uptake of O_2 and the evolution of CO_2 (photorespiration) (Canvin, 1990). The pivotal role of catalase in the in vivo detoxification of photorespiratory H_2O_2 in peroxisomes became obvious in the work of Kendall et al. (1983). These authors observed that a catalase-deficient mutant of barley grew poorly in normal air, followed by death of the older leaves, but grew well in 0.2% CO_2, a concentration known to largely suppress photorespiration. Here it is shown that Fe excess in leaves of *N. plumbaginifolia* led to a doubling of the catalase activity within 12 h (Fig. 4). However, whether this increase in catalase activity is due to a stimulation of photorespiration by Fe or not needs to be further addressed. In this context it should be kept in mind that we measured total catalase activity (Fig. 4). At least two different catalases (Cat1 and Cat2) seem to contribute to the catalase activity in photosynthetic tissues of *N. plumbaginifolia* (Willekens et al., 1994a). At the moment we do not know whether this observed doubling of catalase activity upon Fe stress is related to increases in Cat1 and/or Cat2.

Whereas Fe excess led to an inhibition of photosynthesis (Fig. 2), the respiration was strongly stimulated under these conditions. This, together with the strongly increased G6PDH activity (Fig. 4), indicated a higher oxidative breakdown of hexoses. Indeed, the Fe-stressed leaves had strongly reduced contents of Glc and Fru compared to the control (Table II). These are most likely adaptations (within 12 h) of the leaf to cope with the Fe-induced cellular damage (Fig. 1) and that deliver NADPH and ATP for anabolic processes. The mitochondrial MnSOD activity of *N. plumbaginifolia* was previously found to parallel closely the activity of the respiratory electron transport chain of mitochondria (Bowler et al., 1989). Also the mRNA level for the FeSOD of *N. plumbaginifolia* has been reported to increase upon chloroplastic stress, e.g. inhibition of photosynthesis by methyl viologen (Tsang et al., 1991). Within 12 h of Fe stress there was no change in total detectable SOD activity or in the amount of MnSOD and FeSOD compared with control leaves (Figs. 4 and 5). However, these results do not necessarily contradict previous findings by Bowler et al. (1989) and Tsang et al. (1991), who reported changes in the expression profiles of different SOD genes only relatively late after different kinds of stress treatments. Based on similar observations in *N. plumbaginifolia* leaves exposed to different stresses such as ozone, SO_2, and UV-B treatment, Willekens et al. (1994b) hypothesized that SODs may be part of the late plant response to an oxidative stress, whereas catalases especially form part of the initial antioxidant response. Whether different SODs are induced after prolonged Fe toxicity has not been investigated so far. There is a need for further investigations of SOD induction to gain deeper insight into the precise timing of the antioxidant response.

A doubling of the endogenous leaf Fe content within 12 h had a dramatic impact on both the visible phenotype and physiology of a higher plant. This is consistent with the hypothesis that Fe uptake will directly generate oxidative stress. A further indication for an Fe-induced oxidative stress was the apparent increased requirement to detoxify H_2O_2 in leaves. Both catalase and AsA peroxidase activities but not the GSH peroxidase activity doubled within 12 h (Fig. 4). Whereas the function of plant GSH peroxidase is still a matter of debate, AsA peroxidase is well known to be important in the detoxification of H_2O_2 (Foyer, 1993). It should be pointed out that the AsA peroxidase activity also exists in compartment-specific isoforms (chloroplastic and cytosolic) (Foyer, 1993). Currently, we do not know in which compartment the AsA peroxidase activity increased.

AsA peroxidase uses AsA as the electron donor for the reduction of H_2O_2, and the redox pairs DAsA/AsA and GSSG/GSH are intermediate electron carriers in the reduction of H_2O_2 by NADPH (Foyer, 1993). Therefore, we determined the endogenous levels of the antioxidants AsA (Foyer, 1993) and GSH (Rennenberg and Brunold, 1994) and their responses to Fe excess (Table III). To our surprise, both the AsA and GSH contents showed marked variations among individual control plants of up to 2-fold (Table III).

To support the reliability of these results, we determined the recoveries for each metabolite (see "Materials and Methods"). The observation that the AsA pool in leaves of *N. plumbaginifolia* seemed not to be precisely regulated is in marked contrast with other reports (for review, see Foyer, 1993, and refs. therein), indicating that the AsA pool in leaves of higher plants is maintained at a remarkably constant level. Cakmak and Marschner (1992) also reported largely deviating AsA contents in leaves of *Phaseolus vulgaris*. In accordance with other observations (Foyer, 1993; Rennenberg and Brunold, 1994), the GSH/GSSG and AsA/DAsA pairs were strongly reduced in unstressed control leaves (Table III). Both redox pairs responded to the induced Fe excess with a decrease of the reduced form by 30% and an equivalent increase of the oxidized form within 12 h (Table III). This result corresponded very well with the observed doubling of the AsA peroxidase activity (Fig. 4) and further supports the view that Fe toxicity results from an oxidative stress. On the basis of these observations, we favor the following working hypothesis. In unstressed leaves GSH and AsA might be present in a large excess and not serve any apparent function under nonstress conditions; thus their levels must not be precisely regulated. Instead, AsA and GSH may function as a pre-existing buffer system to provide immediately antioxidant power when oxidative stress occurs.

In conclusion, if a doubling of the leaf Fe content gives rise to severe cellular damage, then the intracellular amount of Fe must be finely regulated and precisely adapted to the cellular demands. Further studies are needed to pinpoint how higher plants sense the intracellular Fe status and whether plants repress the uptake system and/or induce detoxification mechanisms in response to a surplus of Fe. Detailed studies will be needed to evaluate how excess Fe leads to the toxicity phenotype described here.

ACKNOWLEDGMENTS

We would like to thank Dr. Ekkehard Neuhaus (University of Osnabrück, Germany) for his very helpful advice and for stimulating discussions. We thank Dr. Alex De Meyer for help with the Fe determination. Help by Karel Spruyt with the photos and Martine De Cock with preparing the manuscript is gratefully acknowledged.

Received August 8, 1994; accepted November 21, 1994.

LITERATURE CITED

Arnon DI (1949) Copper enzymes in isolated chloroplasts. Polyphenol oxidase in *Beta vulgaris*. Plant Physiol **24:** 1–15

Beauchamp C, Fridovich I (1971) Superoxide disrnutase: improved assays and an assay applicable to acrylamide gels. Anal Biochem **44:** 276–287

Beyer WF, Fridovich I (1987) Assaying for superoxide dismutase activity: some large consequences of minor changes in conditions. Anal Biochem **161:** 559–566

Björkman O, Powles SB (1984) Inhibition of photosynthetic reactions under water stress: interaction with light level. Planta **161:** 490–504

Bowler C, Alliotte T, De Loose M, Van Montagu M, Inzé D (1989) The induction of manganese superoxide dismutase in response to stress in *Nicotiana plumbaginifolia*. EMBO J **8:** 31–38

Bowler C, Van Montagu M, Inzé D (1992) Superoxide dismutase and stress tolerance. Annu Rev Plant Physiol Plant Mol Biol **43:** 83–116

Braun V, Hantke K (1990) Genetics of bacterial iron transport. *In* G Winkelmann, ed, Handbook of Microbial Iron Chelates. CRC Press, Boca Raton, FL, pp 107–138

Cakmak I, Marschner H (1992) Magnesium deficiency and high light intensity enhance activities of superoxide dismutase, ascorbate peroxidase, and glutathione reductase in bean leaves. Plant Physiol **98:** 1222–1227

Canvin DT (1990) Photorespiration and CO_2-concentrating mechanisms. *In* DT Dennis, DH Turpin, eds, Plant Physiology, Biochemistry and Molecular Biology. Longman Scientific & Technical, Burnt Mill, UK, pp 253–273

Chaney RL, Brown JC, Tiffin LO (1972) Obligatory reduction of ferric chelates in iron uptake by soybeans. Plant Physiol **50:** 208–213

Dancis A, Roman DG, Anderson GJ, Hinnebusch AG, Klausner RD (1992) Ferric reductase of *Saccharomyces cerevisiae*: molecular characterization, role in iron uptake, and transcriptional control by iron. Proc Natl Acad Sci USA **89:** 3869–3873

Drotar A, Phelps P, Fall R (1985) Evidence for glutathione peroxidase activities in cultured plant cells. Plant Sci **42:** 35–40

Fee JA (1991) Regulation of *sod* genes in *Escherichia coli*: relevance to superoxide dismutase function. Mol Microbiol **5:** 2599–2610

Foyer C, Lelandais M, Galap C, Kunert KJ (1991) Effects of elevated cytosolic glutathione reductase activity on the cellular glutathione pool and photosynthesis in leaves under normal and stress conditions. Plant Physiol **97:** 863–872

Foyer CH (1993) Ascorbic acid. *In* RG Alscher, JL Hess, eds, Antioxidants in Higher Plants. CRC Press, Boca Raton, FL, pp 31–58

Foyer CH, Lescure J-C, Lefebvre C, Morot-Gaudry J-F, Vincentz M, Vaucheret H (1994) Adaptations of photosynthetic electron transport, carbon assimilation, and carbon partitioning in transgenic *Nicotiana plumbaginifolia* plants to changes in nitrate reductase activity. Plant Physiol **104:** 171–178

Giannopolitis CN, Ries SK (1977) Superoxide dismutases. I. Occurrence in higher plants. Plant Physiol **59:** 309–314

Graeve K, von Schaewen A, Scheibe R (1994) Purification, characterization, and cDNA sequence of glucose-6-phosphate dehydrogenase from potato (*Solanum tuberosum* L.). Plant J **5:** 353–361

Griffith OW (1980) Determination of glutathione and glutathione disulfide using glutathione reductase and 2-vinylpyridine. Anal Biochem **106:** 207–212

Guinel FC, LaRue TA (1990) Formation of wall appositions in leaves and lateral roots of an iron-accumulating pea mutant. Can J Bot **68:** 1340–1348

Halliwell B, Gutteridge JMC (1984) Oxygen toxicity, oxygen radicals, transition metals and disease. Biochem J **219:** 1–14

Hipkins MF, Baker NR (1986) Photosynthesis: Energy Transduction; A Practical Approach. IRL Press, Oxford, UK

Johnson HS (1972) Dithiothreitol: an inhibitor of glucose-6-phosphate dehydrogenase activity in leaf extracts and isolated chloroplasts. Planta **106:** 273–277

Jungmann J, Reins H-A, Lee J, Romeo A, Hassett R, Kosman D, Jentsch S (1993) MAC1, a nuclear regulatory protein related to Cu-dependent transcription factors is involved in Cu/Fe utilization and stress resistance in yeast. EMBO J **12:** 5051–5056

Kammler M, Schön C, Hantke K (1993) Characterization of the ferrous iron uptake system of *Escherichia coli*. J Bacteriol **175:** 6212–6219

Kampfenkel K (1992) Limited proteolysis of NADP-malate dehydrogenase from pea chloroplast by aminopeptidase K yields monomers. Evidence of proteolytic degradation of NADP-malate dehydrogenase during purification from pea. Biochim Biophys Acta **1156:** 71–77

Kampfenkel K, Braun V (1993) Topology of the ExbB protein in the cytoplasmic membrane of *Escherichia coli*. J Biol Chem **268:** 6050–6057

Kendall AC, Keys AJ, Turner JC, Lea PJ, Miflin BJ (1983) The isolation and characterization of a catalase-deficient mutant of barley (*Hordeum vulgare*). Planta **159:** 505–511

Klapheck S, Zimmer I, Cosse H (1990) Scavenging of hydrogen peroxide in the endosperm of *Ricinus communis* by ascorbate peroxidase. Plant Cell Physiol **31:** 1005–1013

Kneen BE, LaRue TA, Welch RM, Weeden NF (1990) Pleiotropic effects of *brz*. Plant Physiol **93:** 717–722

Neuhaus HE, Kruckeberg AL, Feil R, Stitt M (1989) Reduced-activity mutants of phosphoglucose isomerase in the cytosol and chloroplast of *Clarkia xantiana*. Planta **178:** 110–122

Neuhaus HE, Stitt M (1989) Perturbation of photosynthesis in spinach leaf discs by low concentrations of methyl viologen. Planta **179:** 51–60

Neuhaus HE, Stitt M (1991) Inhibition of photosynthetic sucrose synthesis by imidodiphosphate, an analog of inorganic pyrophosphate. Plant Sci **76:** 49–55

Okamura M (1980) An improved method for the determination of L-ascorbic acid and L-dehydrosascorbic acid in blood plasma. Clin Chim Acta **103:** 259–268

Quick WP, Stitt M (1989) An examination of factors contributing to non-photochemical quenching of chlorophyll fluorescence in barley leaves. Biochim Biophys Acta **977:** 287–296

Raguzzi F, Lesuisse E, Crichton RR (1988) Iron storage in *Saccharomyces cerevisiae*. FEBS Lett **231:** 253–258

Rennenberg H, Brunold C (1994) Significance of glutathione metabolism in plants under stress. *In* HD Behnke, U Lüttge, K Esser, JW Kadereit, M Runge, eds, Progress in Botany, Vol 55. Springer-Verlag Berlin

Schreiber U, Schliwa U, Bilger W (1986) Continuous recording of photochemical and non-photochemical fluorescence quenching with a new type of modulation fluorimeter. Photosynth Res **10:** 51–61

Smith PK, Krohn RI, Hermanson GT, Mallia AK, Gartner FH, Provenzano MD, Fujimoto EK, Goeke NM, Olson BJ, Klenk DC (1985) Measurement of protein using bicinchoninic acid. Anal Biochem **150:** 76–85

Sonnewald U, Brauer M, von Schaewen A, Stitt M, Willmitzer L (1991) Transgenic tobacco plants expressing yeast-derived invertase in either the cytosol, vacuole or apoplast: a powerful tool for studying sucrose metabolism and sink/source interactions. Plant J **1:** 95–106

Stitt M, Lilley RMcC, Gerhardt R, Heldt HW (1989) Metabolite levels in specific cells and subcellular compartments of plant leaves. Methods Enzymol **174:** 518–552

Tsang EWT, Bowler C, Hérouart D, Van Camp W, Villarroel R, Genetello C, Van Montagu M, Inzé D (1991) Differential regulation of superoxide dismutases in plants exposed to environmental stress. Plant Cell **3:** 783–792

Welch RM, LaRue TA (1990) Physiological characteristics of Fe accumulation in the 'Bronze' mutant of *Pisum sativum* L., cv 'Sparkle' E107 (*brz brz*). Plant Physiol **93:** 723–729

Willekens H, Langebartels C, Tiré C, Van Montagu M, Inzé D, Van Camp W (1994a) Differential regulation of catalase gene expression in *Nicotiana plumbaginifolia* L. Proc Natl Acad Sci USA **91:** 10450–10454

Willekens H, Van Camp W, Van Montagu M, Inzé D, Sandermann H Jr, Langebartels C (1994b) Ozone, sulfur dioxide, and ultraviolet B have similar effects on mRNA accumulation of antioxidant genes in *Nicotiana plumbaginifolia*. Plant Physiol **106:** 1007–1014